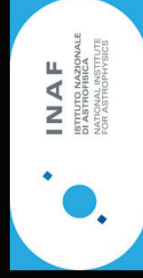


Clustering, lensing and ISW/RS from the DEMNIUni simulations

Carmelita Carbone

INAF - Astronomical Observatory of Brera



*Illuminating Dark energy with the next
generation of cosmological redshift surveys*

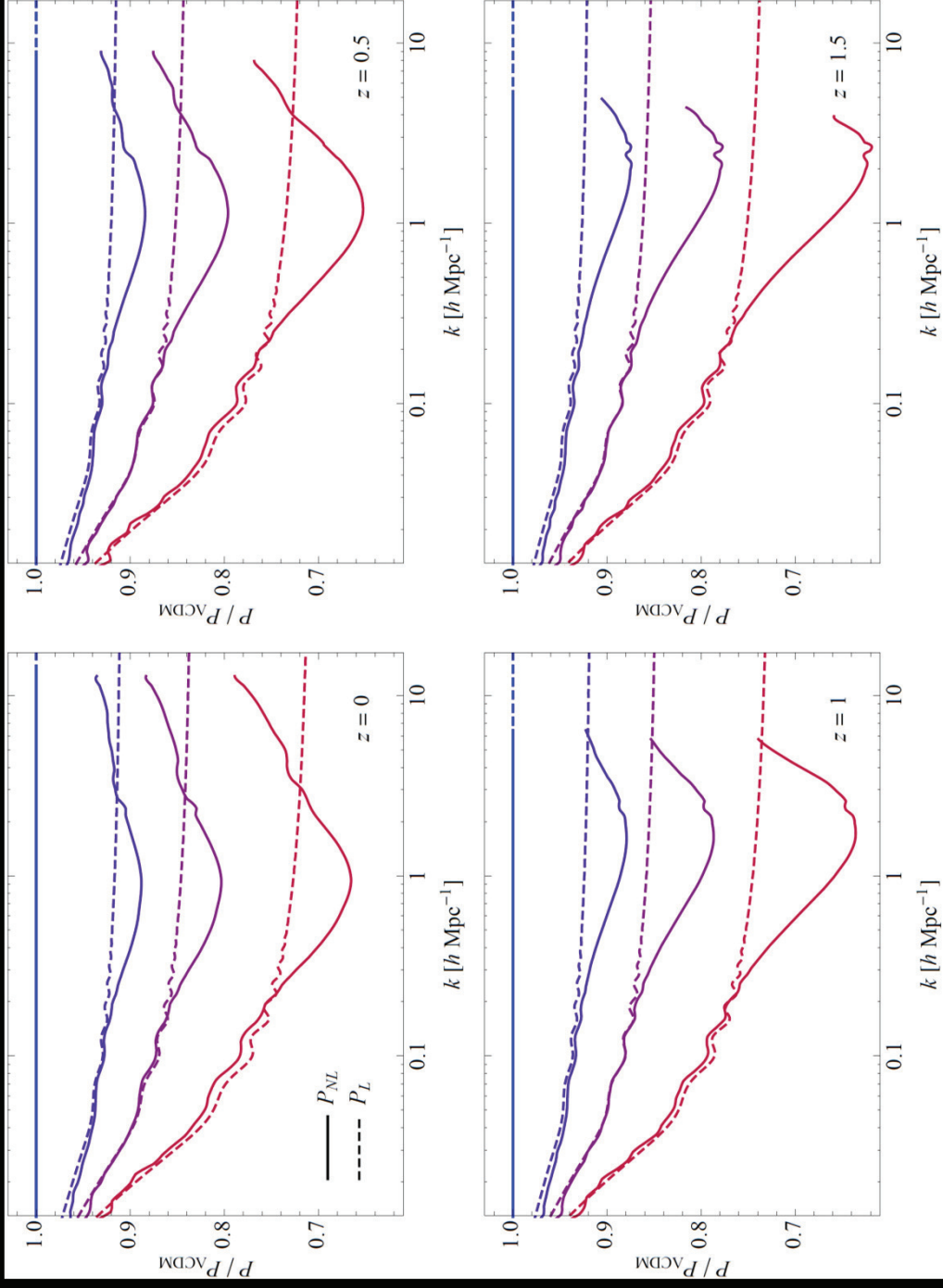


ICTP, May 15th, 2015, Trieste, Italy

Outline

- DEMNUni: Dark Energy and Massive Neutrino Universe simulations
- “DEMNUi: The clustering of large-scale structures in the presence of massive neutrinos”, Castorina et al 2015, in prep
- “DEMNUi: ISW, Rees-Sciama, and weak-lensing in the presence of massive neutrinos”, Carbone et al 2015, in prep

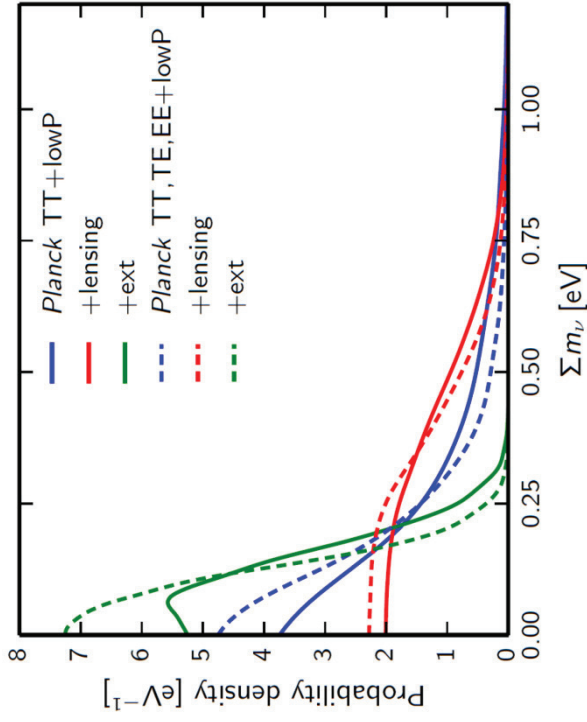
Total matter $P(k)$ ratios with respect to Λ CDM



$$k_{\text{fs}}(z) = 0.82H(z)/H_0/(1+z)^2 (m_{\nu}/\text{eV})^2 h \text{ Mpc}^{-1}$$

Planck constraints on neutrinos (95% CL)

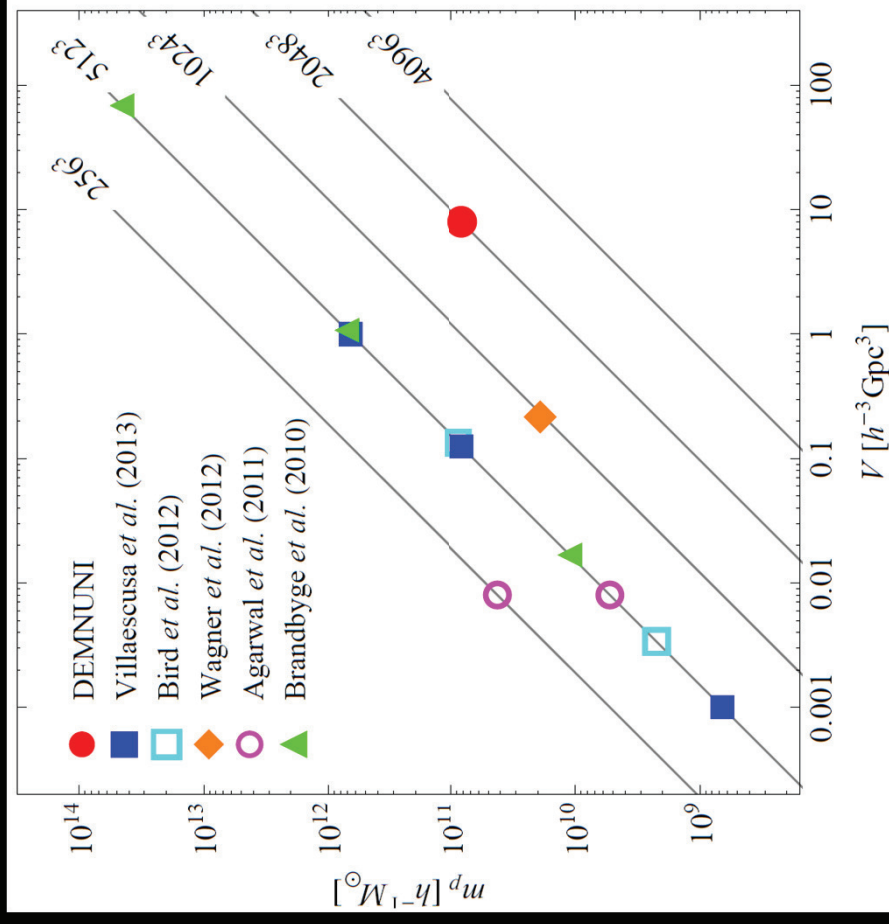
| Parameter | TT | TT+lensing | TT+lensing+ext | TT, TE, EE | TT, TE, EE+lensing | TT, TE, EE+lensing+ext |
|---------------------|----------------------------|----------------------------|-------------------------------|----------------------------|----------------------------|------------------------------|
| Ω_K | $-0.052^{+0.049}_{-0.055}$ | $-0.005^{+0.016}_{-0.017}$ | $-0.0001^{+0.0054}_{-0.0052}$ | $-0.040^{+0.038}_{-0.041}$ | $-0.004^{+0.015}_{-0.015}$ | $0.0008^{+0.0040}_{-0.0039}$ |
| Σm_ν [eV] | < 0.715 | < 0.675 | < 0.234 | < 0.492 | < 0.589 | < 0.194 |
| N_{eff} | $3.13^{+0.64}_{-0.63}$ | $3.13^{+0.62}_{-0.61}$ | $3.15^{+0.41}_{-0.40}$ | $2.99^{+0.41}_{-0.39}$ | $2.94^{+0.38}_{-0.38}$ | $3.04^{+0.33}_{-0.33}$ |
| Y_p | $0.252^{+0.041}_{-0.042}$ | $0.251^{+0.040}_{-0.039}$ | $0.251^{+0.035}_{-0.036}$ | $0.250^{+0.026}_{-0.027}$ | $0.247^{+0.026}_{-0.027}$ | $0.249^{+0.025}_{-0.026}$ |
| $dn_s/d \ln k$ | $-0.008^{+0.016}_{-0.016}$ | $-0.003^{+0.015}_{-0.015}$ | $-0.003^{+0.015}_{-0.014}$ | $-0.006^{+0.014}_{-0.014}$ | $-0.002^{+0.013}_{-0.013}$ | $-0.002^{+0.013}_{-0.013}$ |
| $r_{0.002}$ | < 0.103 | < 0.114 | < 0.114 | < 0.0987 | < 0.112 | < 0.113 |
| w | $-1.54^{+0.62}_{-0.50}$ | $-1.41^{+0.64}_{-0.56}$ | $-1.006^{+0.085}_{-0.091}$ | $-1.55^{+0.58}_{-0.48}$ | $-1.42^{+0.62}_{-0.56}$ | $-1.019^{+0.075}_{-0.080}$ |



Planck-XIII (2015): the lensing reconstruction data, which directly probes the lensing power, prefers lensing amplitudes slightly below (but consistent with) the base Λ CDM prediction. The Planck+lensing constraint therefore pulls the constraints slightly away from zero towards higher neutrino masses. Extending the analysis up to $L < 900$, Planck lensing gives a detection for the neutrino mass:

$$\sum m_\nu = 0.16^{+0.08}_{-0.11} \text{ eV} \quad (\text{Planck TT+lowP+aggressive lensing + BAO; 68\%})$$

Castorina, CC et al in prep



Comparison between the DEMNUNI runs and previous, recent simulations of massive neutrino cosmologies in terms of cold dark matter mass resolution and volume

DEMNUi simulations

- ▶ 5×10^6 cpu-hours on BGQ/FERMI at CINECA
- ▶ 4 mixed dark matter cosmological simulations for CMB and LSS analysis in the presence of massive neutrinos
- ▶ Planck cosmology, $M_\nu=0, 0.17, 0.3, 0.53$ eV
- ▶ Gadget-3 with ν -particle component (Viel et al. 2010)
- ▶ box-size size: 2 Gpc/h
- ▶ particle number: 2×2048^3 (CDM+ ν)
- ▶ CDM mass: $8 \times 10^{10} M_\odot/h$ (neutrino particle mass depends on M_ν)
- ▶ softening length: 20 kpc/h
- ▶ starting redshift: $z_{\text{in}}=99$

$$k_{\text{nr}} = 0.018(m_\nu/1\text{eV})^{1/2}\Omega_m^{1/2}h/\text{Mpc}$$

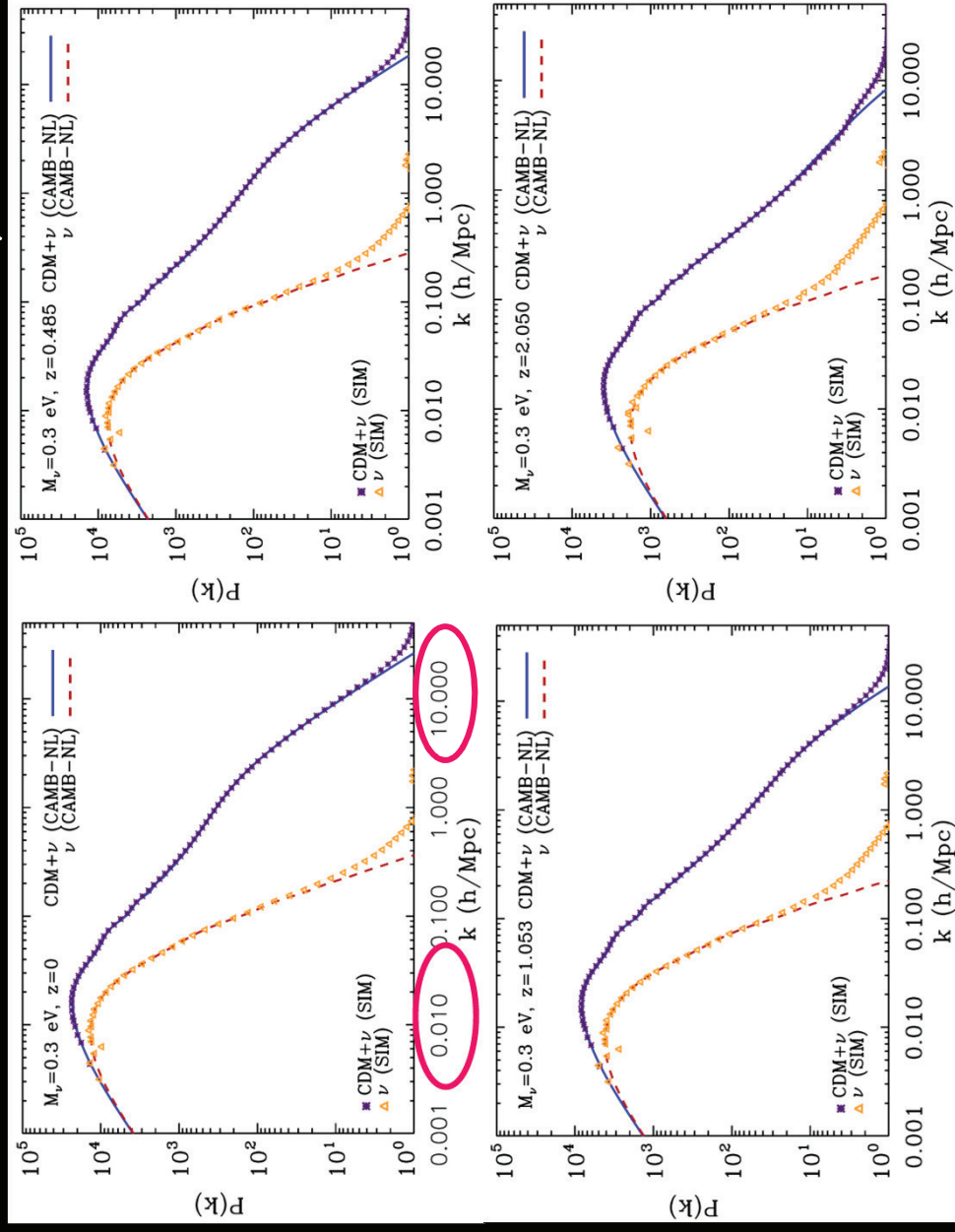
Simulation outputs

- **62 temporary snapshots per simulation: ~0.54 TB/snap (CDM+ v)**
- **62 halo-catalogs**
- **62 sub-halo catalogs**
- **Matter power-spectra and correlation functions for all the 62 snapshots**
- **50 temporary gravitational potential grids of size 4096^3 (for CMB weak-lensing)**
- **50 temporary grids of size 4096^3 for the derivative of the gravitational potential (for ISW/Rees-Sciama)**

DEMNUi collaboration

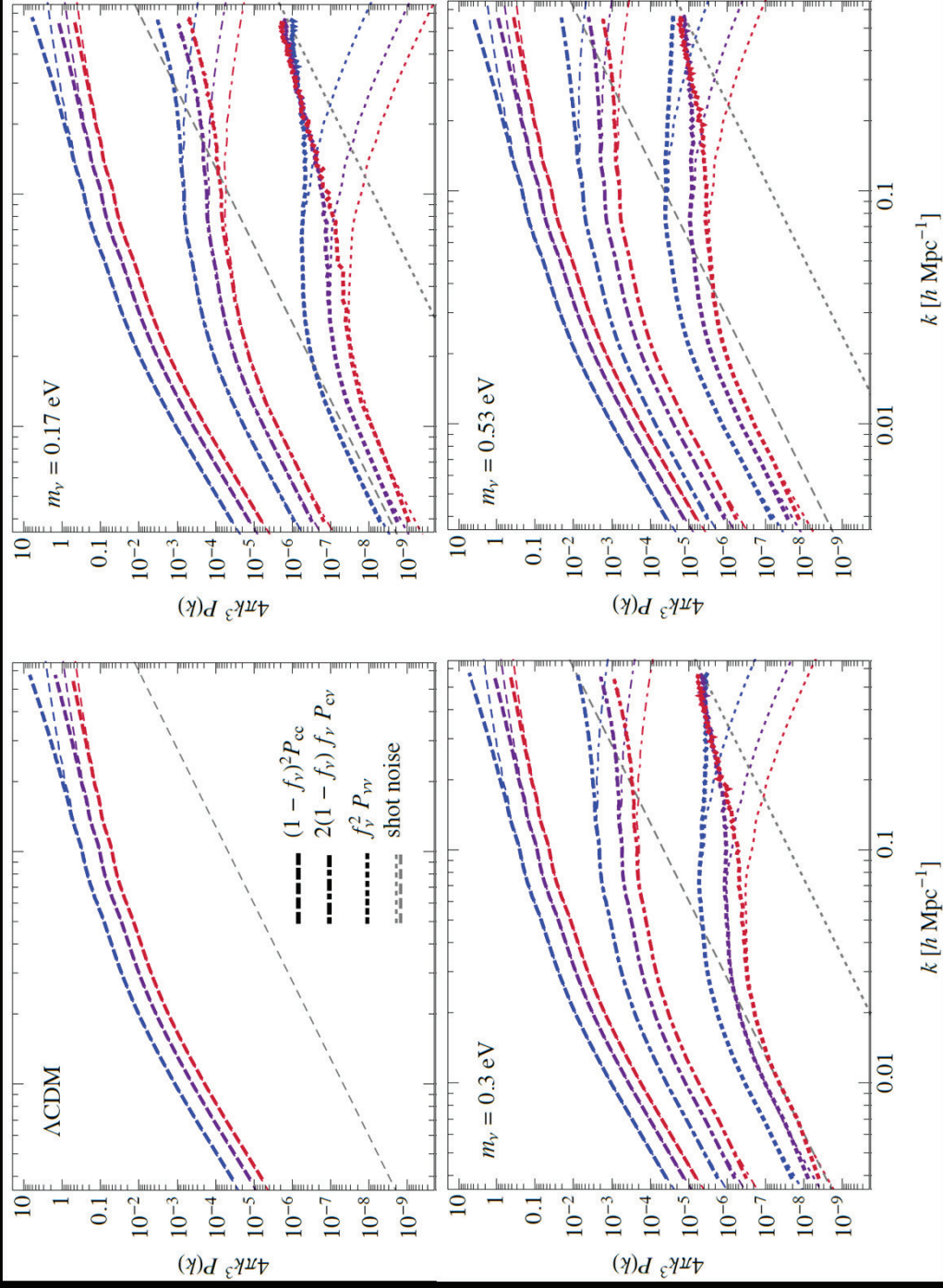
- **P-Gadget3 code with massive neutrinos: M. Viel**
- **Simulation runs: C. Carbone (PI), K. Dolag**
- **CMB-lensing and ISW/Rees-Sciama maps: C. Carbone, M. Petkova**
- **Galaxy clustering: E. Castorina, M. Zennaro, J. Bel, D. Bianchi, E. Sefusatti**
- **HOD with massive neutrinos: A. J. Hawken**
- **SZ-maps and cross-correlation with lensing: M. Roncarelli, C. Giocoli, C. Carbone**
- **Convergence maps and cross-correlation with ISW/RS: C. Carbone , C. Giocoli**
- **High-order statistics: M. Moresco, J. Bel, E.Sefusatti**
- **Voids with massive neutrinos: A. J. Hawken, C. Carbone, B. Granett, A. Iovino**

DEMNUni matter power spectra for $M_\nu=0.3$ eV



The large volume of the DEMNUni simulation suite allows to measure the power spectrum in neutrino cosmologies at the 1% level on the scales characterised by BAO, allowing a test of perturbation theory predictions at the level of accuracy required by current and futures galaxy surveys.

Different contributions to the total matter $P(k)$

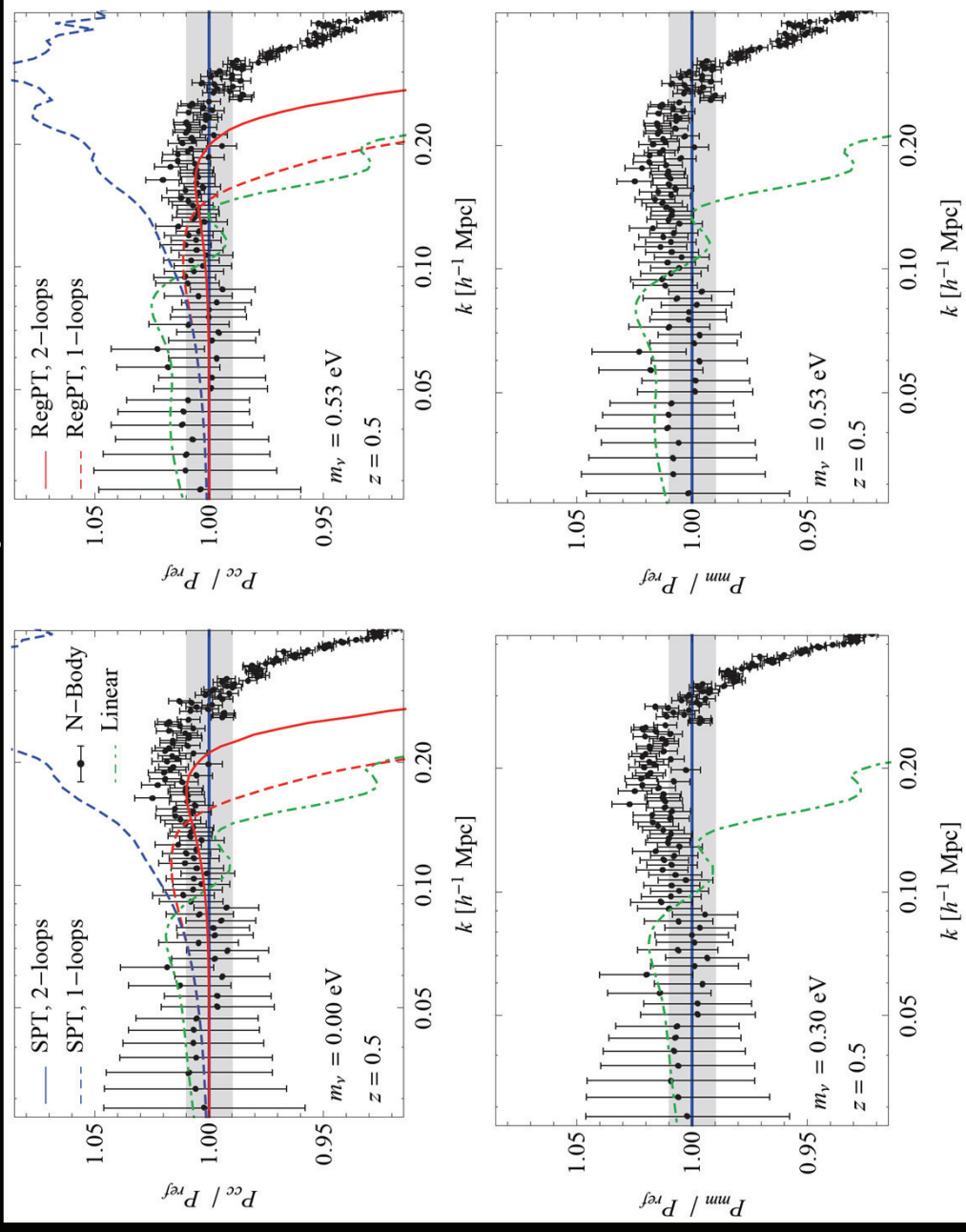


$$P_m(k; z) = (1 - f_\nu)^2 P_{cb}(k; z) + 2(1 - f_\nu) f_\nu P_{cb, \nu}(k; z) + f_\nu^2 P_\nu(k; z)$$

$P_m(k)$ is described at the 1% level assuming the nonlinear evolution of CDM alone, and the linear prediction for the other components

Perturbation theory vs Simulations

Castorina, CC et al in prep

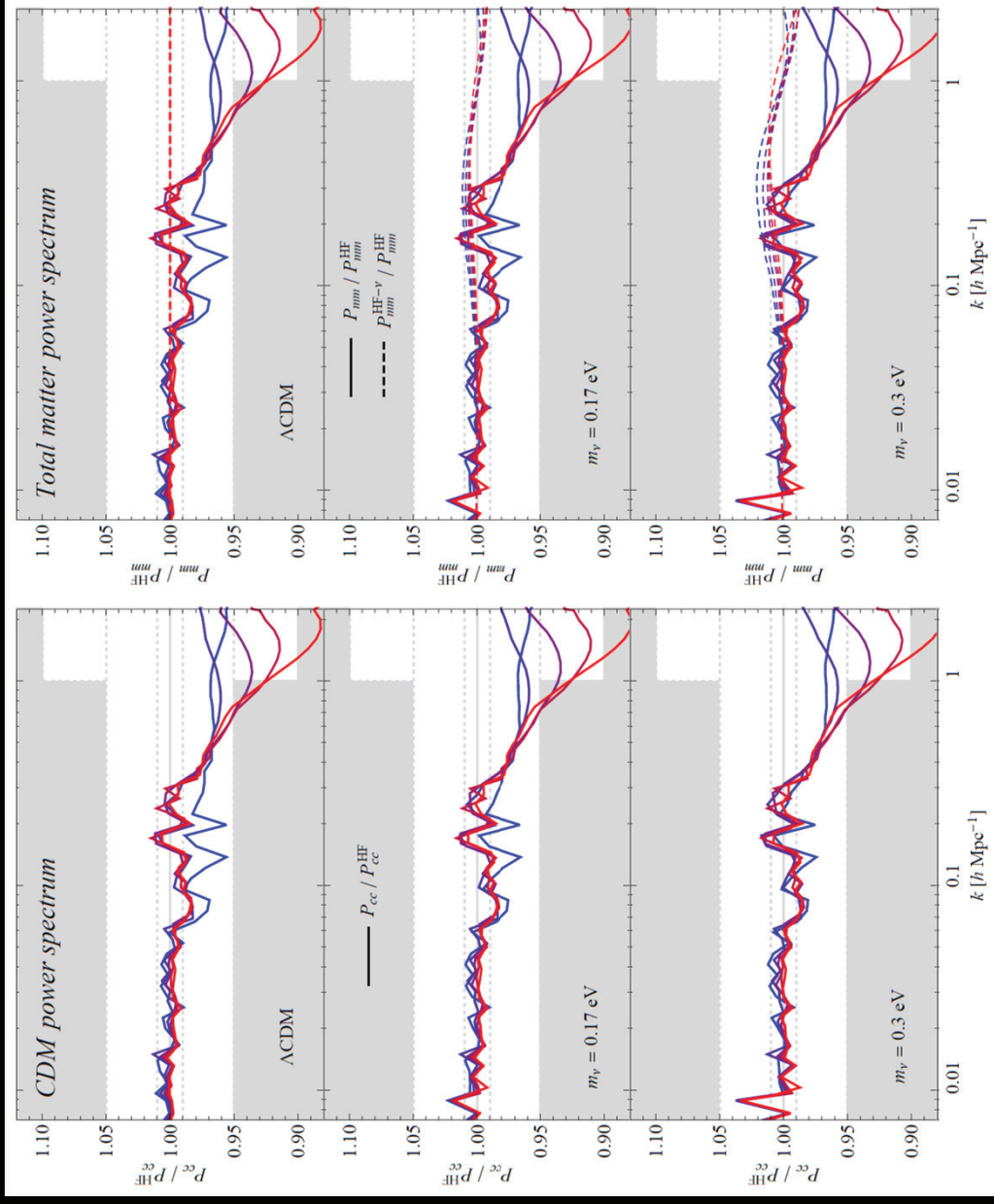


(RegularizedPT: Bernardau et al 2008,
Taruya et al 2012)

$$P_{mm}^{PT}(k) = (1 - f_\nu)^2 P_{cc}^{PT}(k) + 2(1 - f_\nu) f_\nu P_{cv}^L(k) + f_\nu^2 P_{vv}^L(k)$$

Here the neutrino induced scale-dependence is limited to the linear growth factor, $D(k,z)$, while the perturbation kernels are standard ones. PT works better with M_ν

Modifications to Halofit

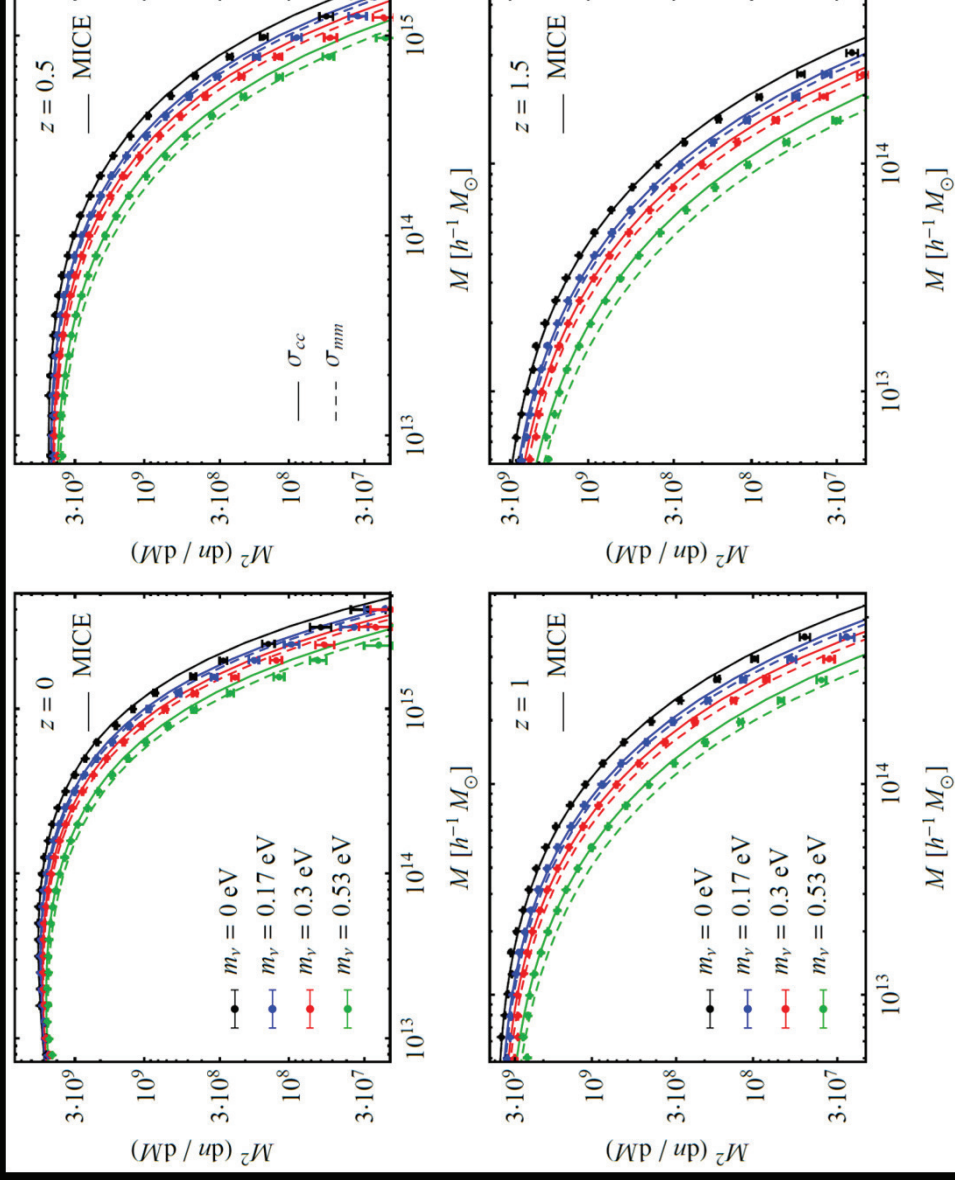


$$P_{mm}^{HF}(k) \equiv (1 - f_\nu)^2 P_{cc}^{HF}(k) + 2f_\nu(1 - f_\nu)P_{c\nu}^L(k) + f_\nu^2 P_{\nu\nu}^L(k)$$

$$P_{cc}^{HF}(k) = \mathcal{F}_{HF}[P_{cc}^L(k)]$$

HALOFIT mapping only for CDM, other contributions are assumed to be linear

Halo Mass Function: FoF

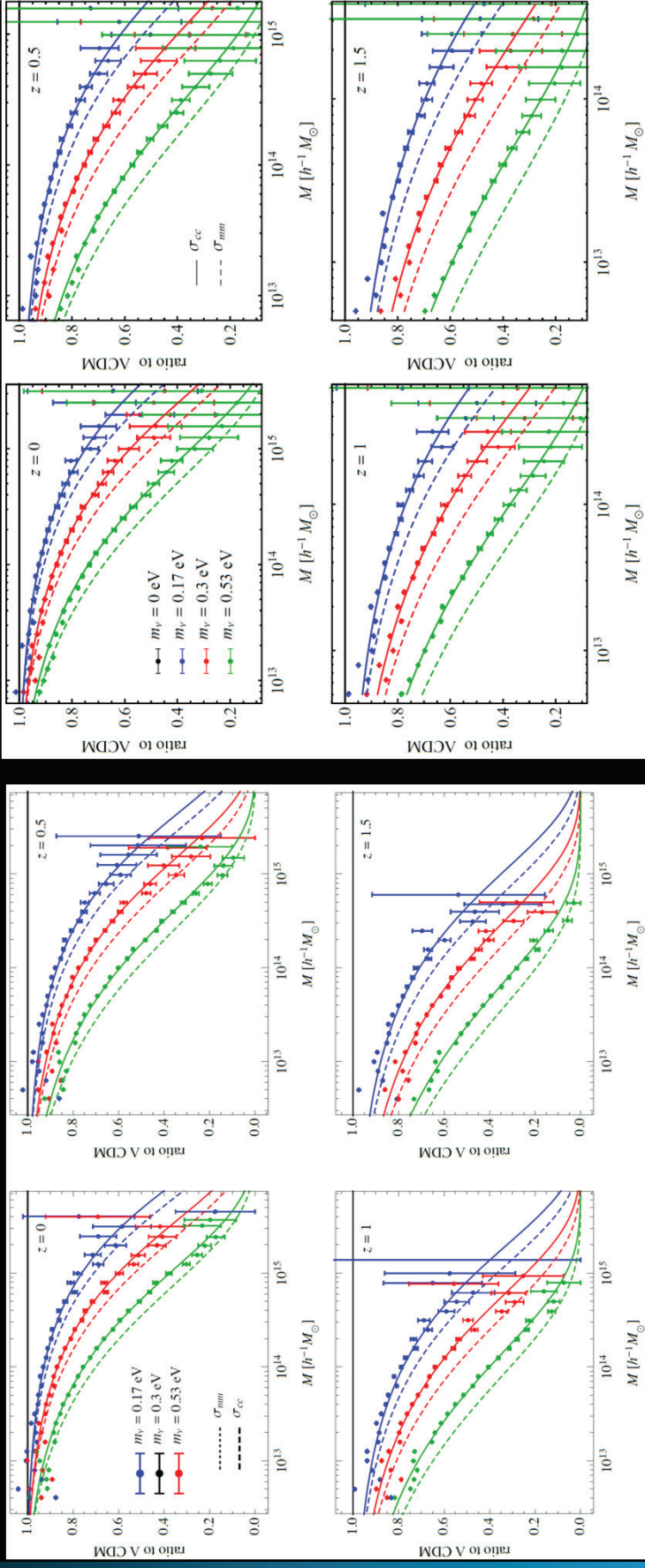


Castorina, CC et al in prep

We recover the ρ_{cc} and σ_{cc} prescription from
Ichiki&Takada (2012) and Castorina et al (2014)

Halo Mass Function: FoF vs SO

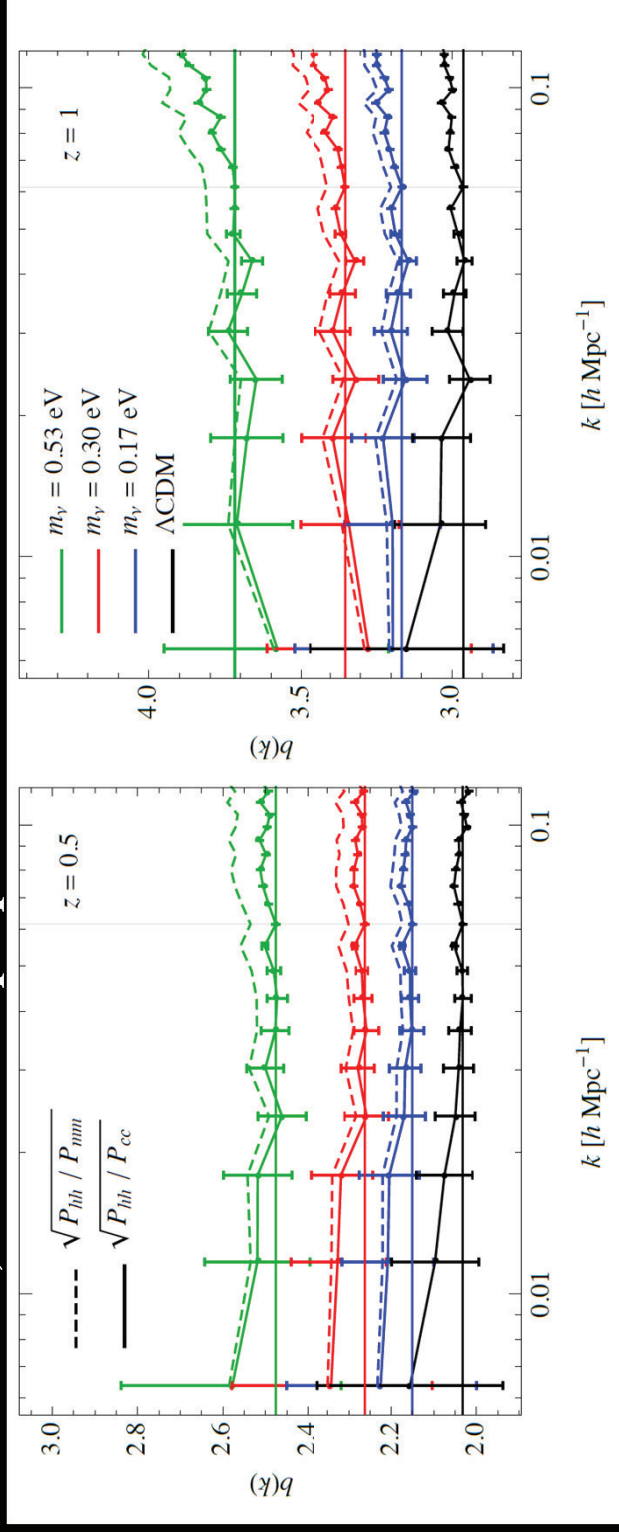
Castorina, CC et al in prep



The ρ_{cc} and σ_{cc} prescriptions allow to recover the theoretical MF for both FoF and SO halos

Analogous conclusions for the bias

Castorina, CC et al in prep



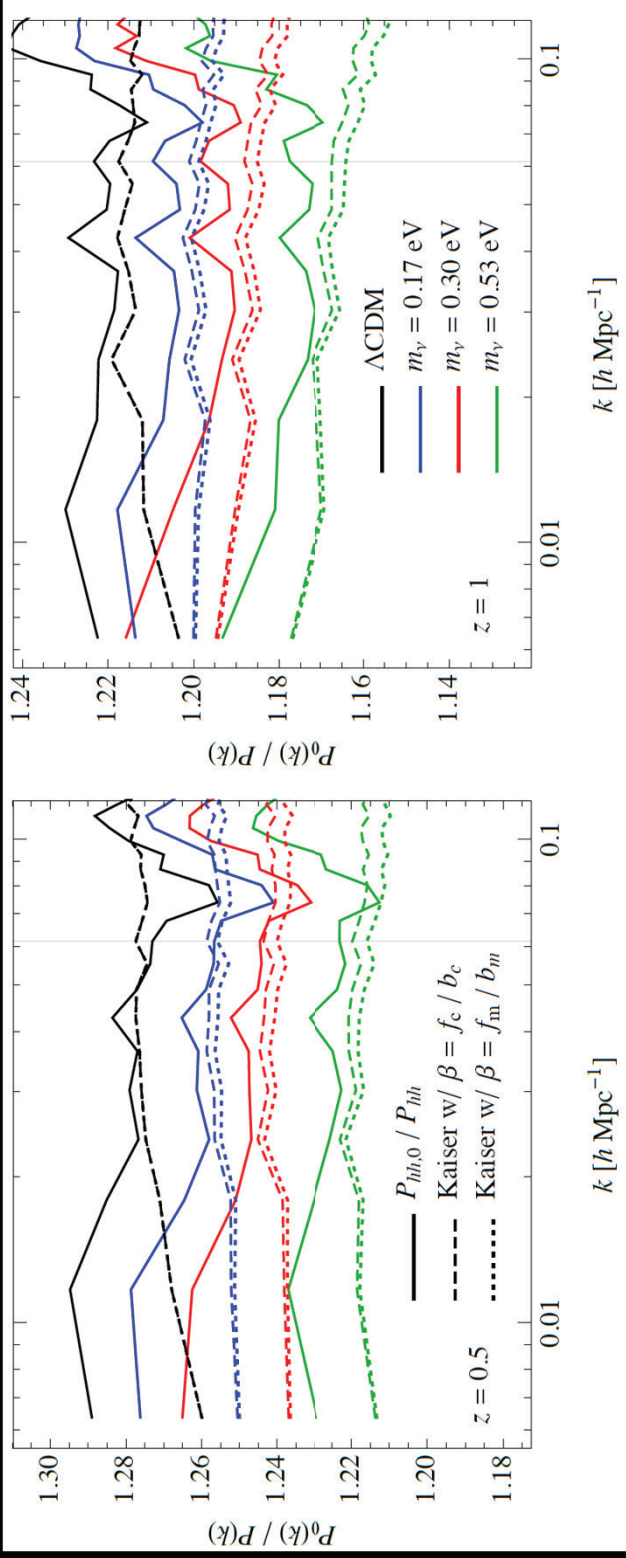
$$b_c = \sqrt{\frac{P_{hh}}{P_{cc}}}$$

$$b_m = \sqrt{\frac{P_{hh}}{P_{mm}}}$$

The σ_{cc} prescription mitigates the ν -induced scale dependence of the bias at intermediate scales. The halo bias defined with respect to DM presents a spurious scale-dependence due to the difference between the cold and total matter power spectra.

Measurements in redshift space

Castorina, CC et al in prep



$$P_{hh,s}(\vec{k}) = (1 + \beta\mu^2)^2 P_{hh}(k) = \sum_{l=0,2,4} P_{hh,\ell} L_\ell(\mu)$$

f_c and σ_{cc} prescriptions work better than f_m and σ_{mm} (velocity bias effects are neglected)

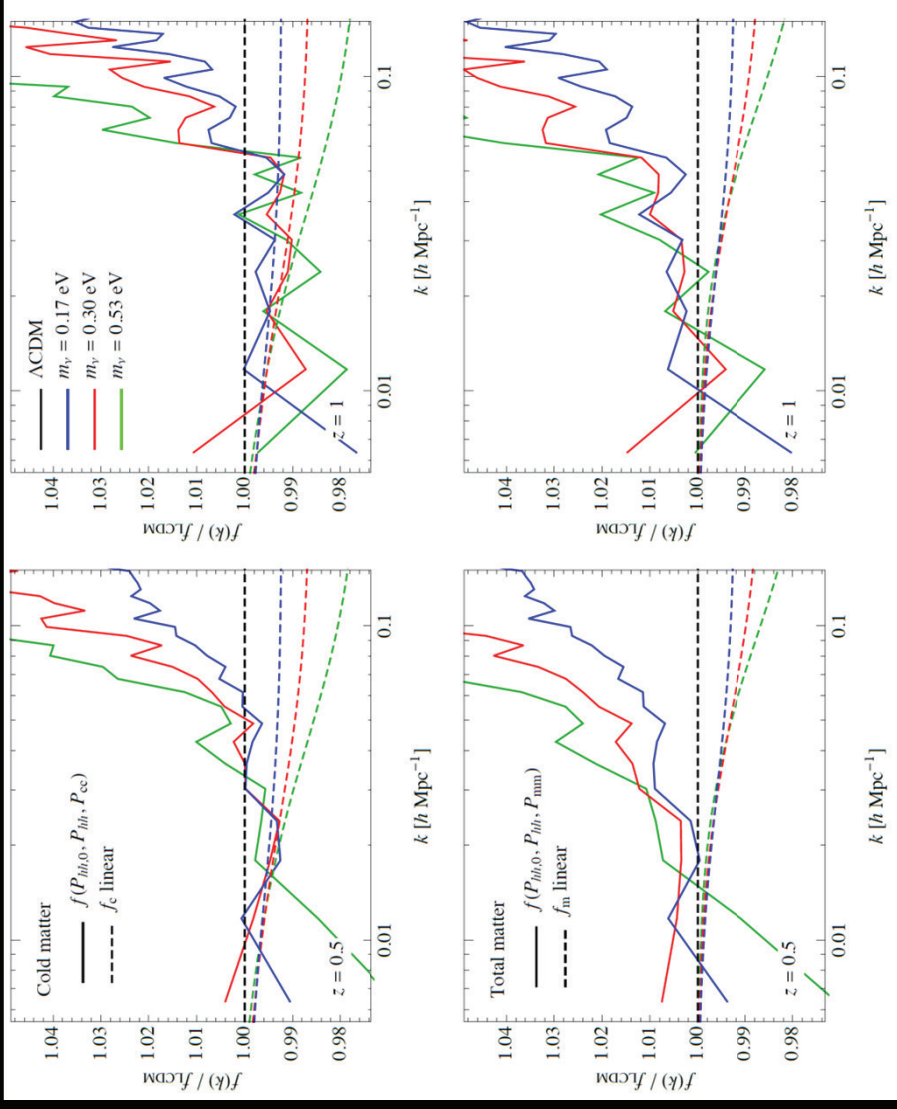
$$P_{hh,0}(k) = \left(1 + \frac{2}{3}\beta + \frac{1}{5}\beta^2\right) P_{hh}(k)$$

$$P_{hh,2}(k) = \left(\frac{4}{3}\beta + \frac{4}{7}\beta^2\right) P_{hh}(k)$$

$$P_{hh,4}(k) = \frac{8}{35}\beta^2 P_{hh}(k),$$

The scale dependent growth-rate

Using b_m instead of b_{cc} implies a systematic error on the determination of the growth rate at the level of 1-2%



$$\beta \equiv f/b$$

$$f(a) \equiv \frac{d \ln D(a)}{d \ln a}$$

$$f(k) = \sqrt{\frac{P_{hh}(k)}{P_{cc}(k)} \frac{1}{3}} \left[\sqrt{45 \frac{P_{hh,0}(k)}{P_{hh}(k)} - 20} - 5 \right]$$

Castorina, CC et al in prep

Lensing and ISW-RS quantities

$$\phi(\hat{n}) = 2 \int dD \frac{(D_s - D)}{DD_s} \Phi(D\hat{n}, D)$$

D = comoving distance
from the observer

Lensing potential in the small-angle
scattering limit (Born approximation)

$$\Delta T(\hat{n}) = \frac{2}{c^3} \bar{T}_0 \int_0^{r_L} \dot{\Phi}(r, \hat{n}) a dr$$

Total ISW-RS effect (only late-ISW)

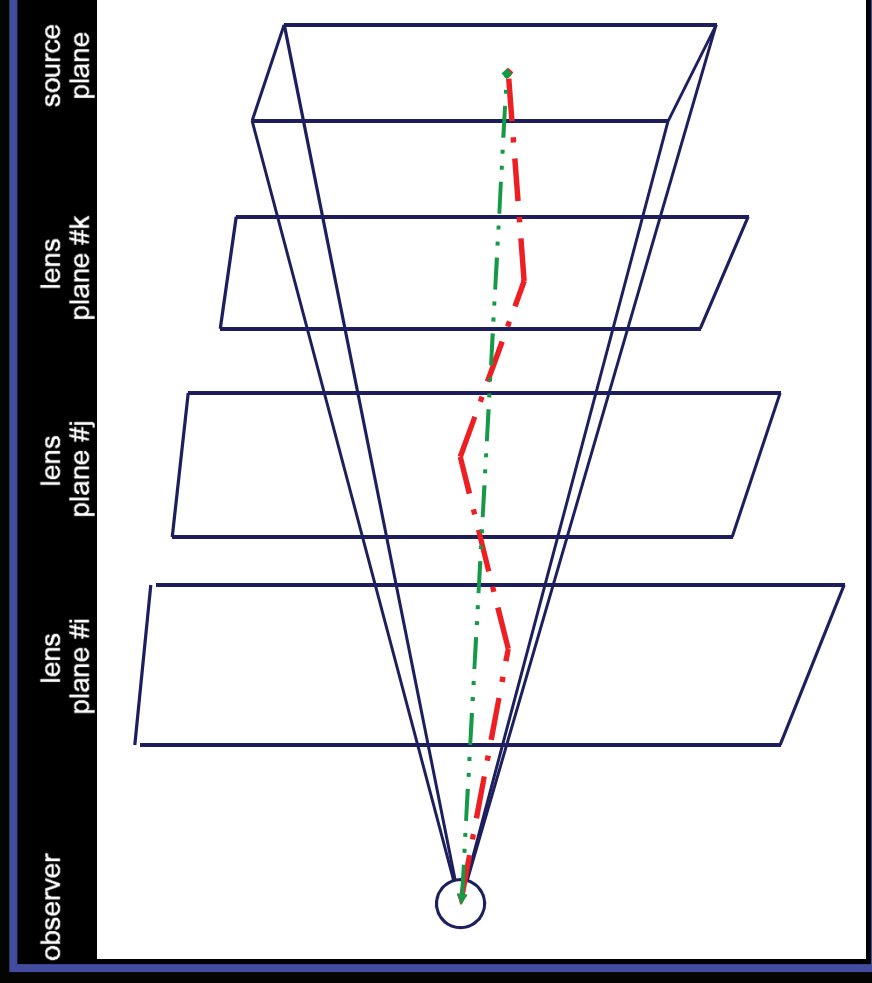
$$\tilde{X}(\hat{n}) = X(\hat{n} + \nabla \phi(\hat{n}))$$

$$X = T, Q, U$$

Gradients in the grav. potential generated by LSS cause deviations in the CMB photon propagation from LS to us:

points in a direction \hat{n} actually come from points on the last scattering surface in a displaced direction $\hat{n}' = \hat{n} + \nabla \phi(\hat{n})$

Weak cosmological lensing and Born approximation

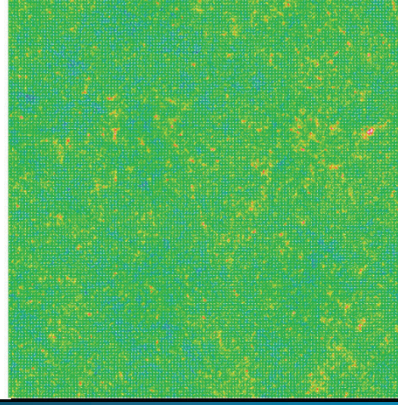
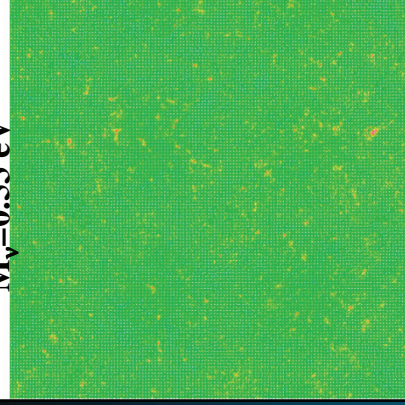


First Born approximation: integration along the undeflected light geodesics.

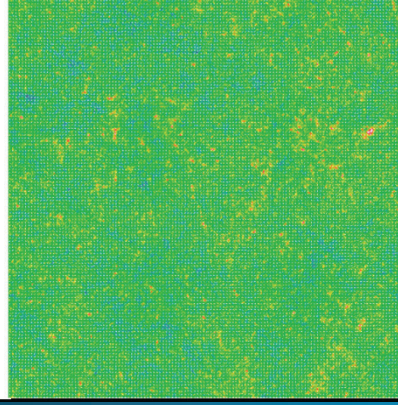
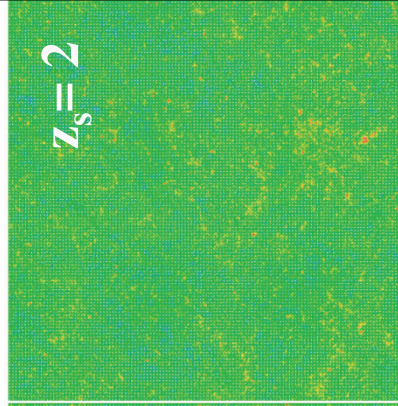
$M_\nu = 0.53 \text{ eV}$

LCDM

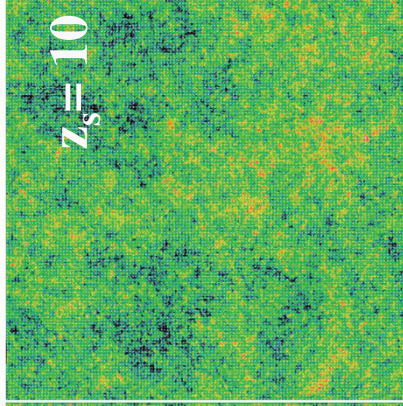
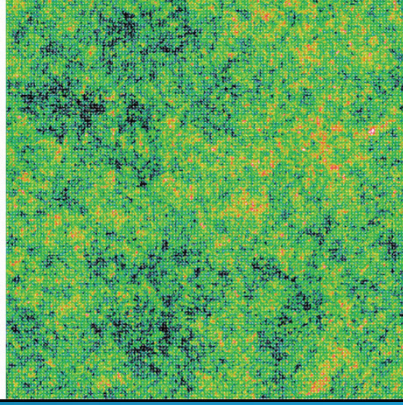
$z_s = 1$



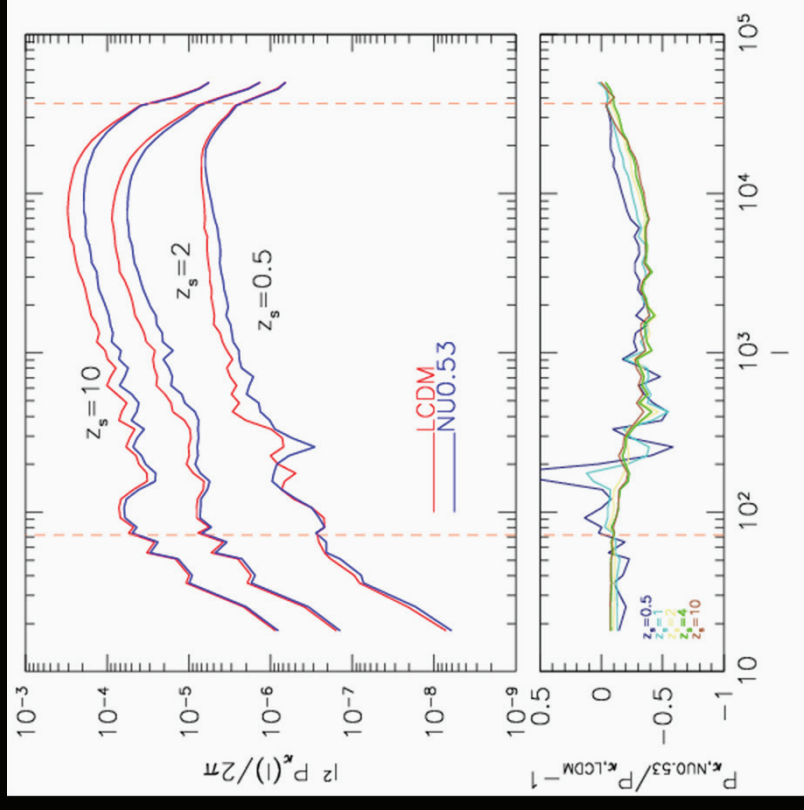
$z_s = 2$



$z_s = 10$

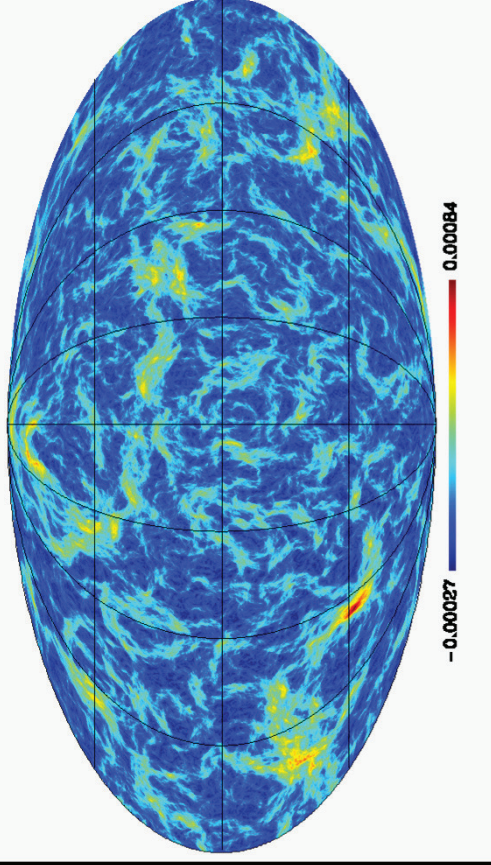


5°x5° converge maps and power-spectra with different source redshift in fla-sky (from C. Giocoli)

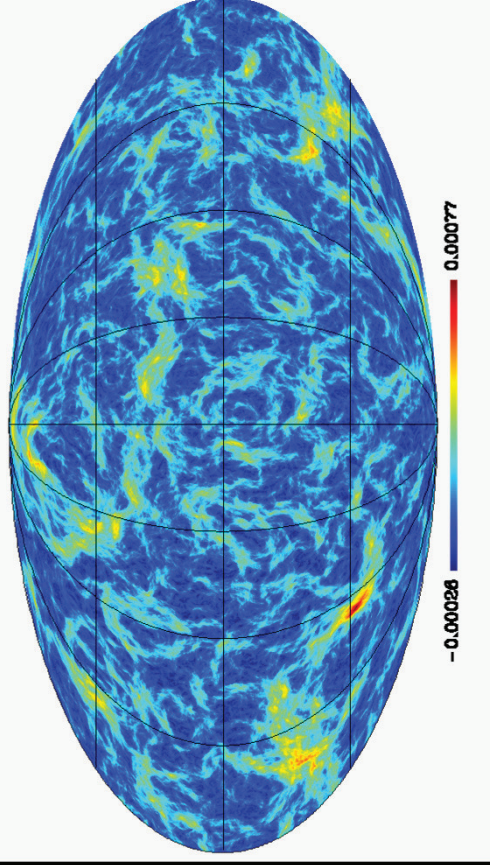


Deflection angle maps for $z_s=1$ (CC et al. in prep)

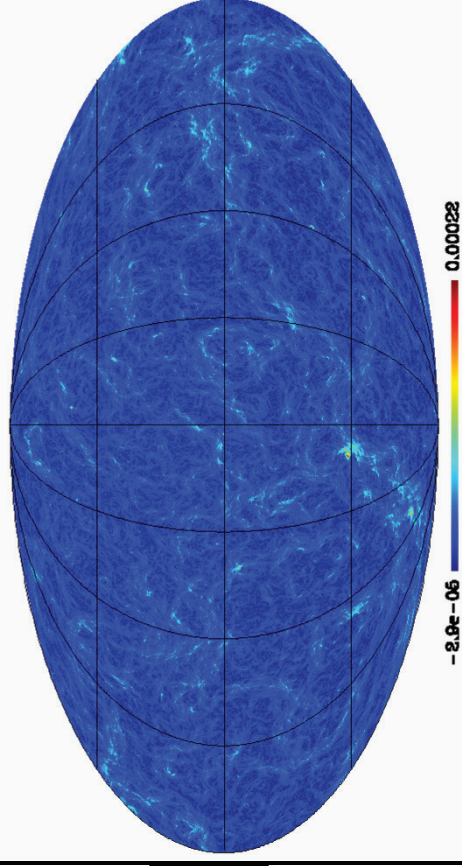
Planck-LCDM weak-lensing α -modulus ($\sigma_8=1$)



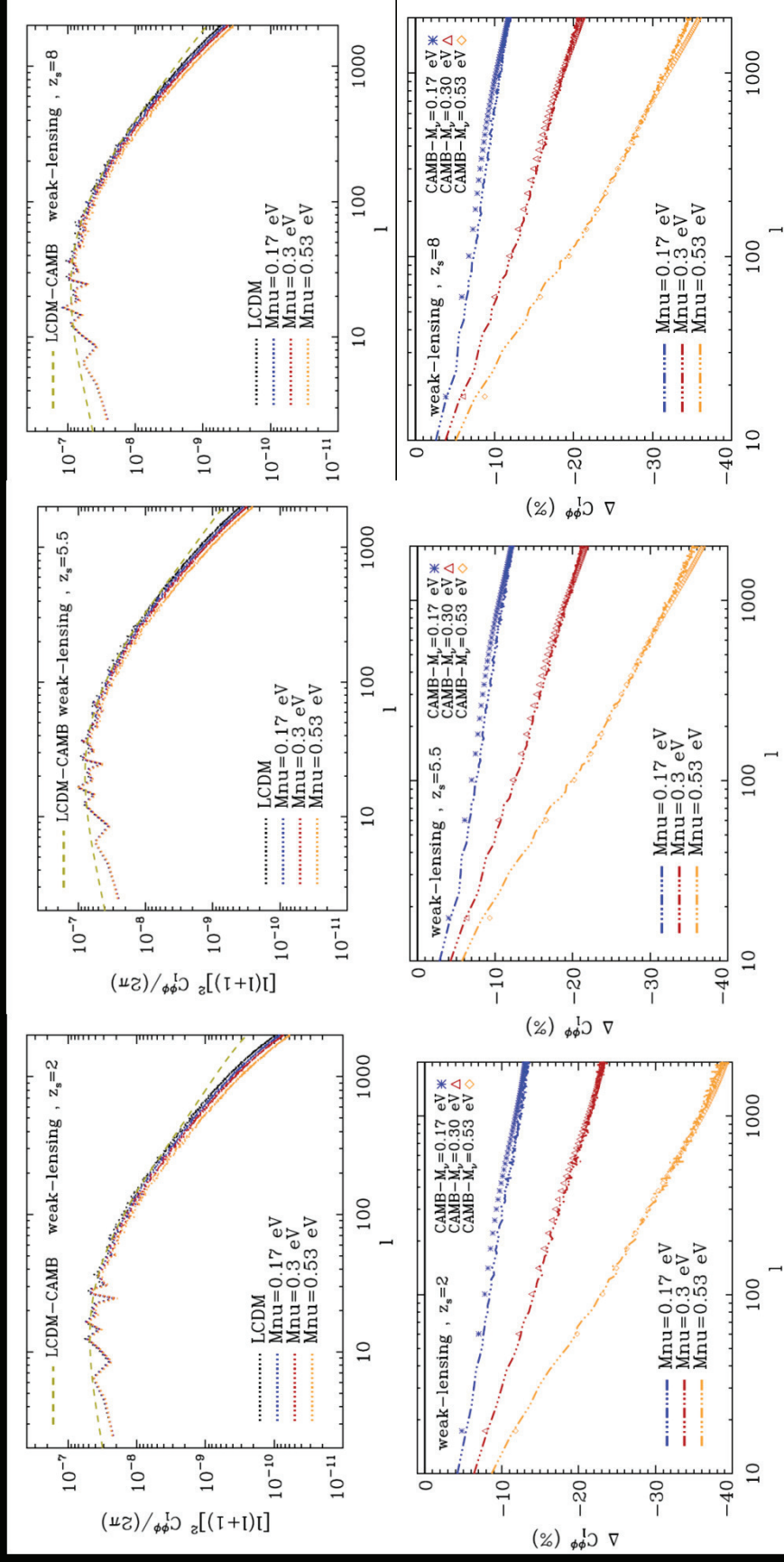
Planck- $M_\nu=0.58$ eV weak-lensing α -modulus ($\sigma_8=1$)



Difference between the LCDM and $M_\nu=0.58$ eV deflections ($\sigma_8=1$)



Weak-lensing angular power spectra at different redshifts



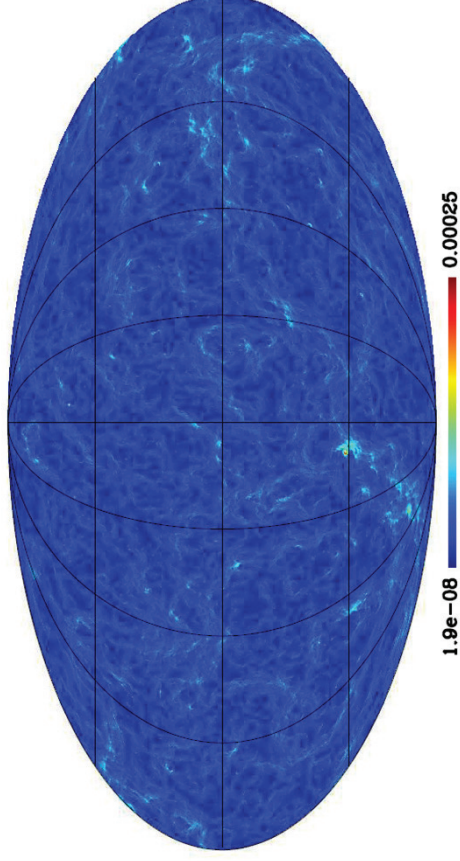
CC et al. in prep

Lack of power on small scales due to grid resolution.
The neutrino damping effect is correctly recovered up to $l=2000$

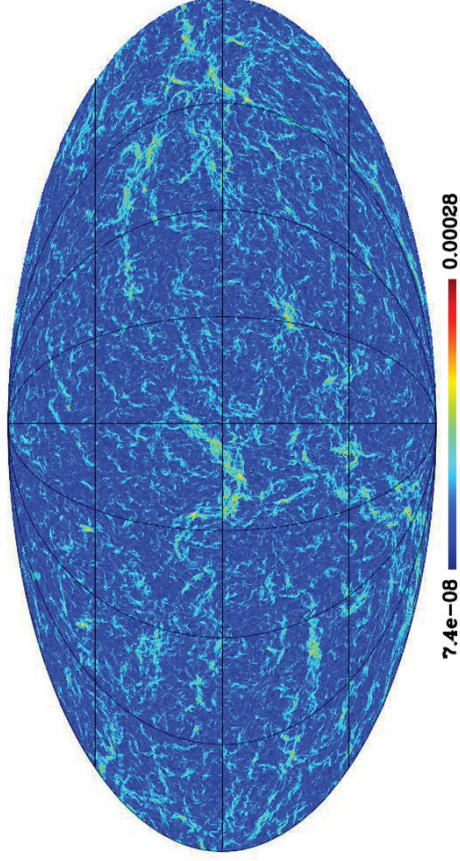
CMB-lensing vs Weak-lensing

CC et al. in prep

Difference between the LCDM and $M_p=0.53$ eV defelections ($z_s=1$)



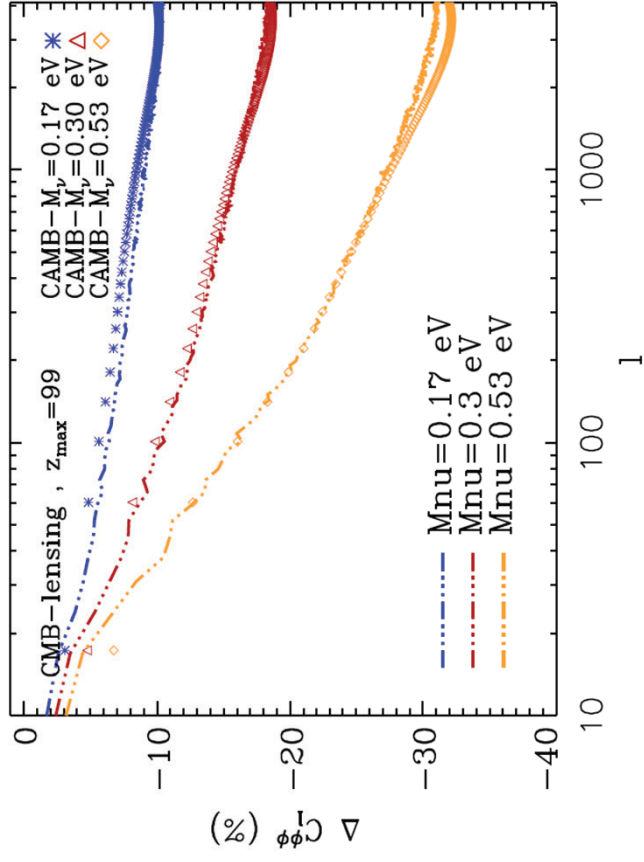
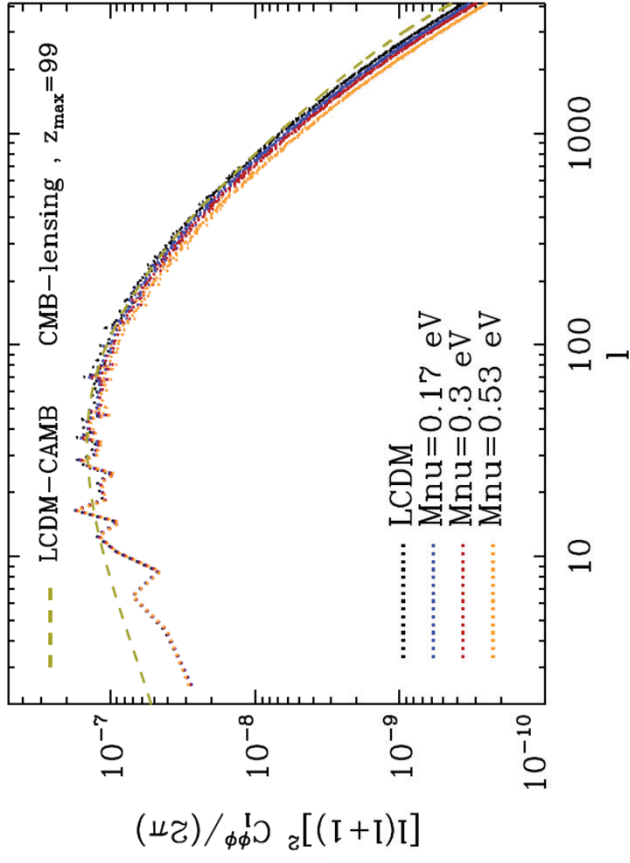
Difference between the LCDM and $M_p=0.53$ eV defelections ($z_s=1100$)



As expected the effect increases with the source redshift

CMB-lensing angular power spectra

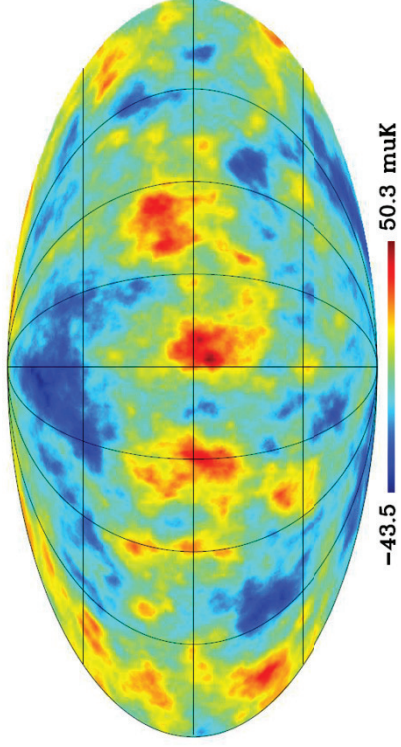
Power suppression is less than in the weak-lensing case since there is the contribution from higher z



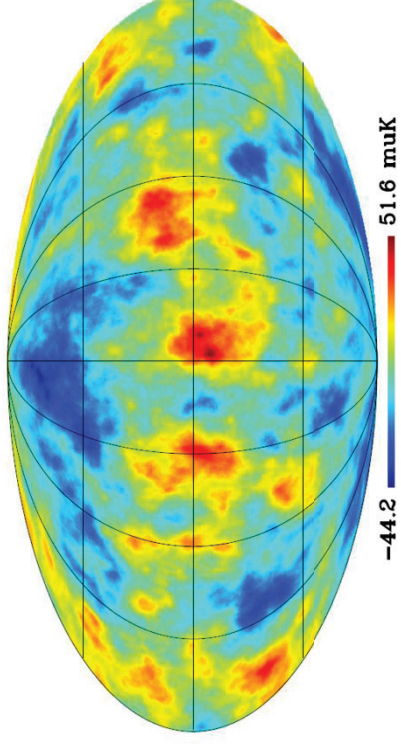
CC et al. in prep

CMB-lensing vs ISW-RS

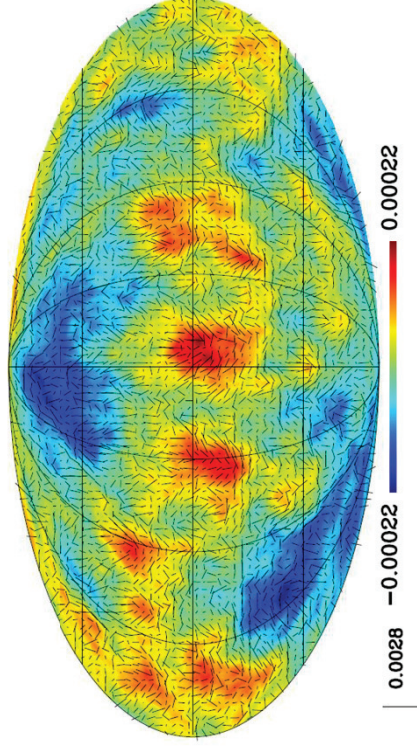
Planck-LCDM ISW/RS map



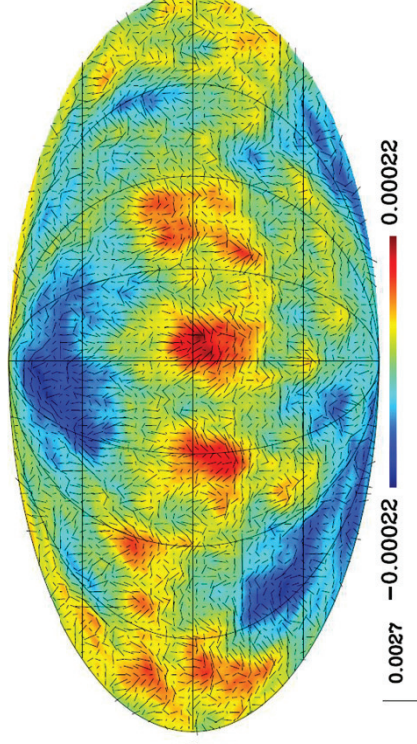
Planck- $M_s=0.53$ eV ISW/RS map



Planck-LCDM CMB-lensing potential map

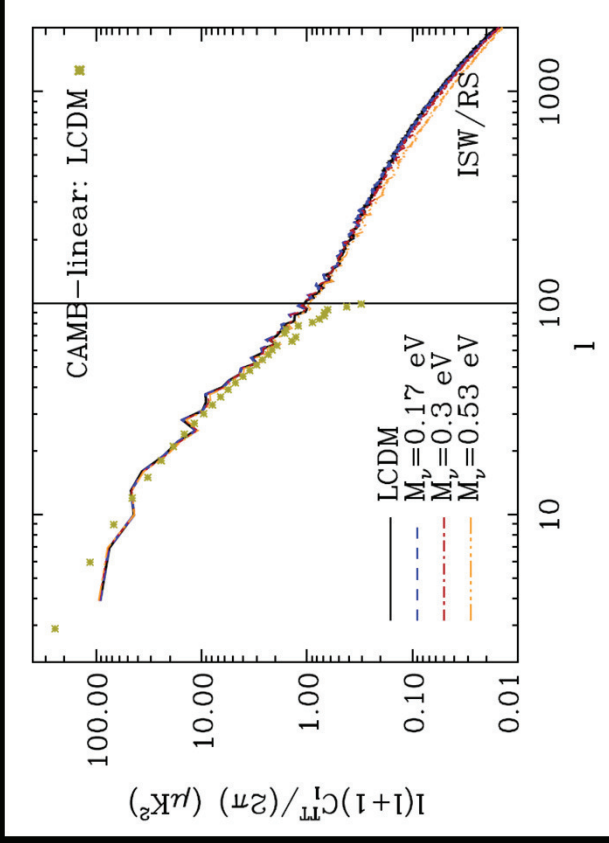


Planck- $M_s=0.53$ eV CMB-lensing potential map

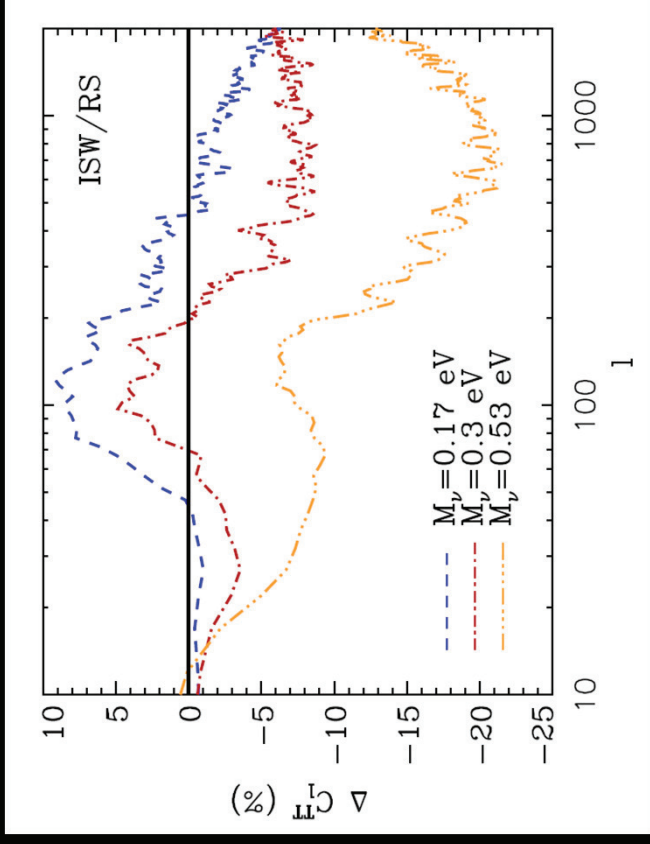


CC et al. in prep

ISWRS angular power spectra

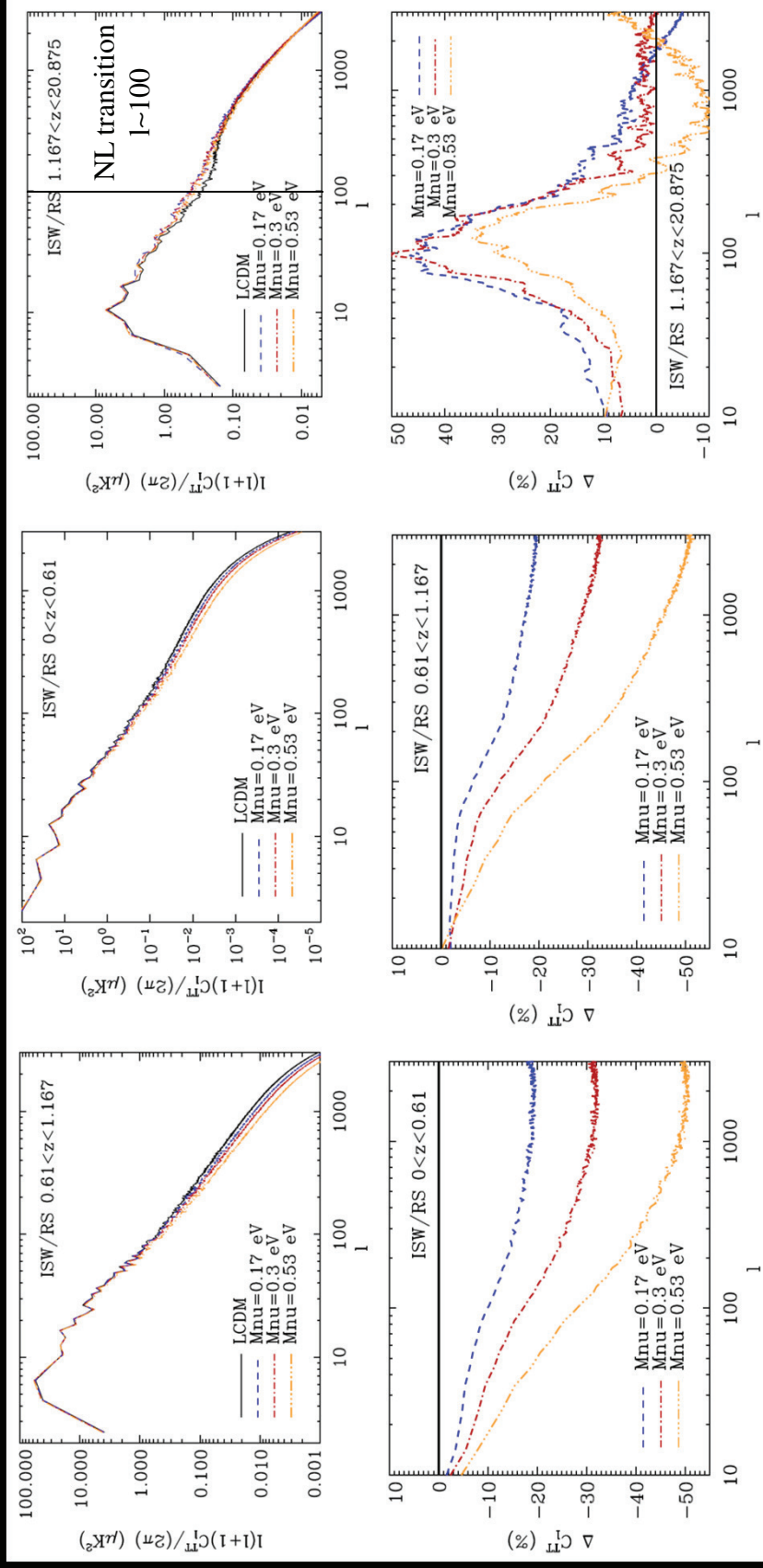


At high redshift, the ISW effect would be null on all scales for $M_\nu=0$, while for $M_\nu>0$ it is still active on small scales because of free-streaming.



CC et al. in prep

ISWRS angular power spectra at different redshifts



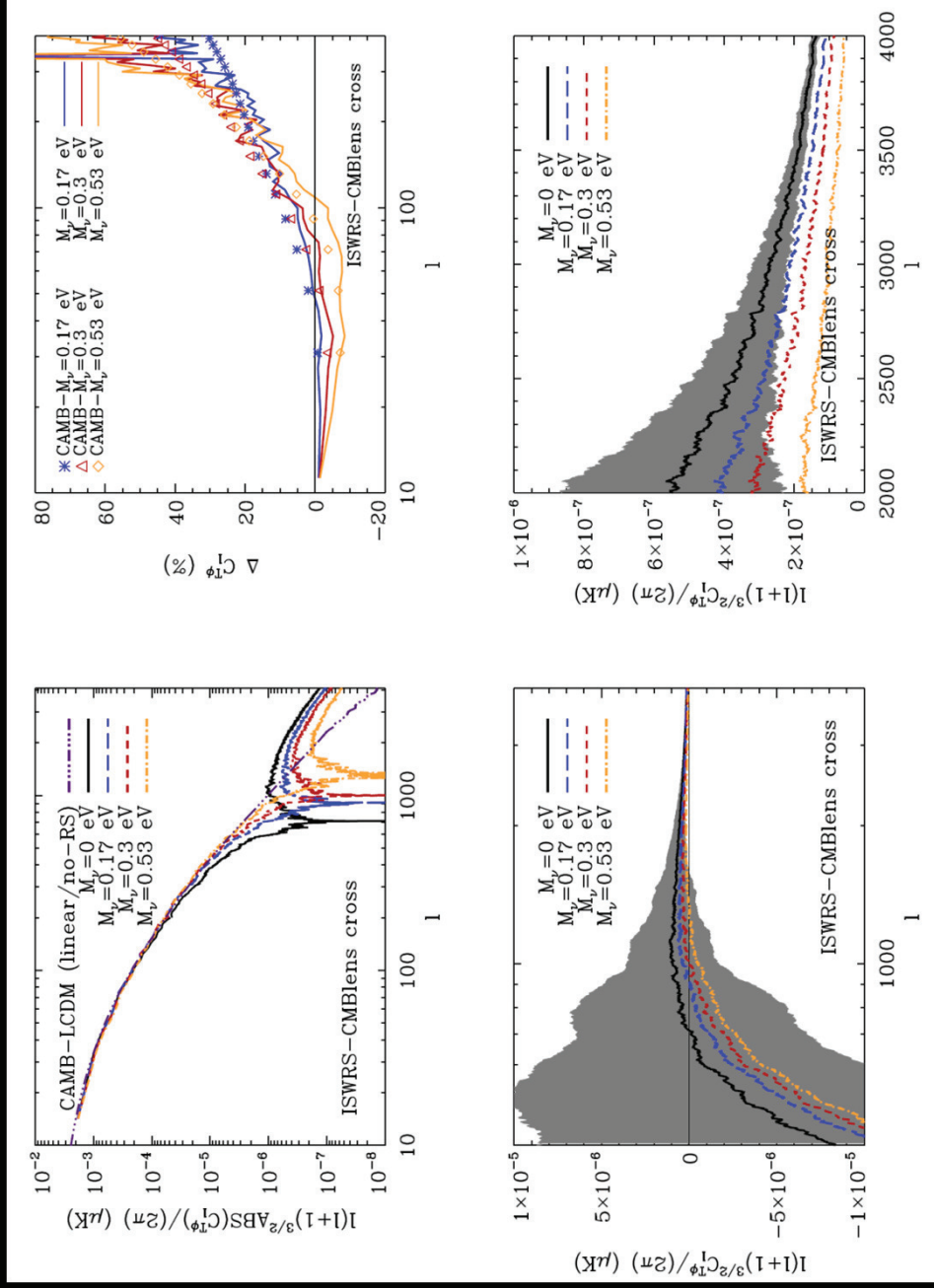
CC et al. in prep

At redshifts non DE-dominated
there is an excess of power

$$k_{\text{fs}}(z) = 0.82H(z)/H_0/(1+z)^2 (m_{\nu}/1\text{eV}) h\text{Mpc}^{-1}$$

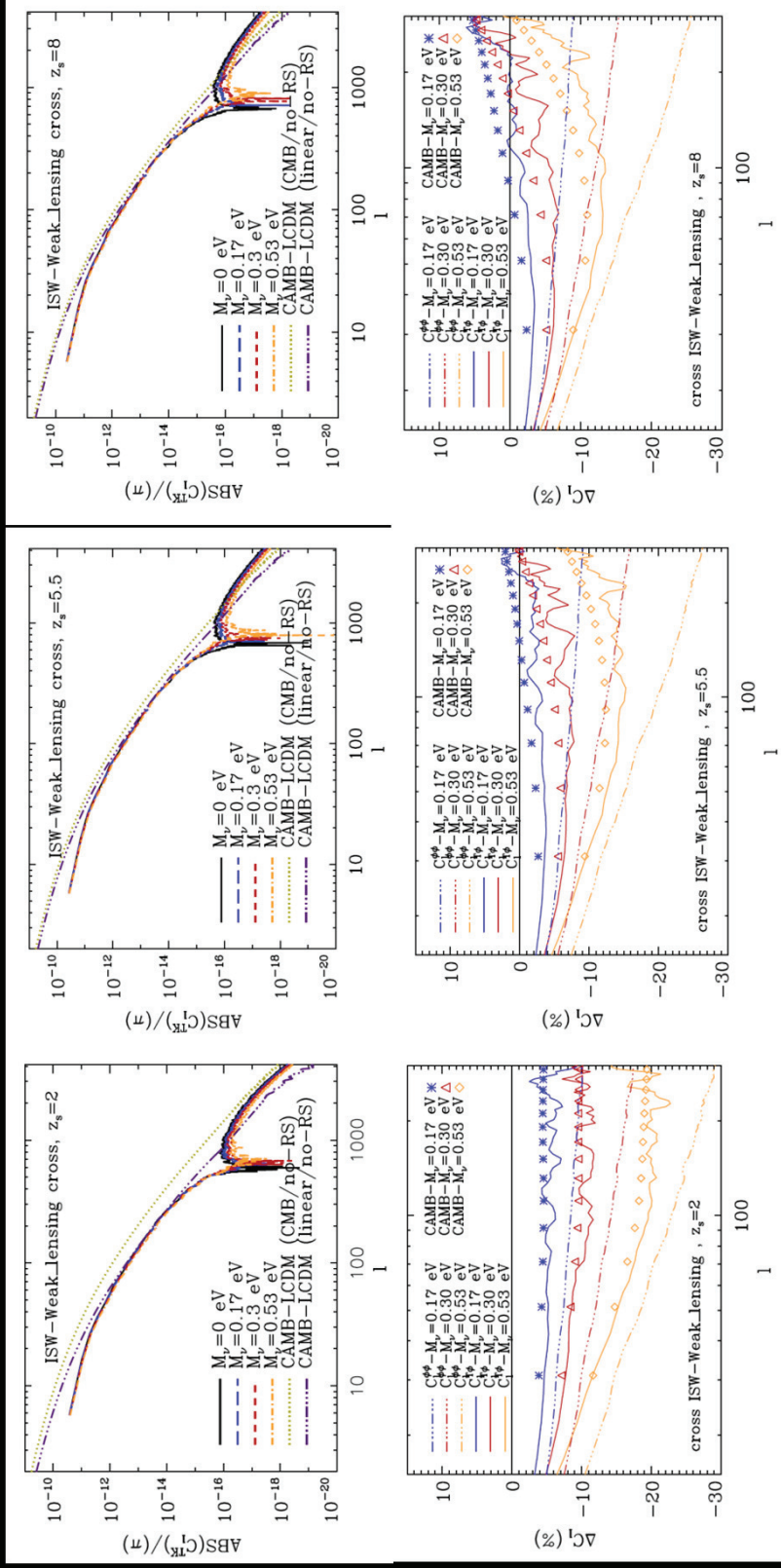
ISWRS-CMB lens cross correlation

CC et al. in prep



Sign inversion: the non-linear transition moves toward smaller scales with increasing neutrino mass

ISWRS-Weakens cross correlation



CC et al. in prep

Difference depends on the source redshift. Excess of power of the cross signal with respect to the auto-correlation signal.

Conclusions

- ✓ **Very large neutrino simulations for different probe combinations**
- ✓ **Previousli results on bias and MF recovered and confirmed**
- ✓ **New Halofit prescription to account for massive neutrinos**
- ✓ **Good behaviour of exiting PT approximations if applied to CDM alone.**
- ✓ **Detection of the scale dependent growth-rate at linear scales**
- ✓ **Suppression of the CMB/weak-lensing signals, depending on the neutrino mass and source redshifts**
- ✓ **Enhancement of power at the ISW-RS transition of about 10% due to neutrino free-streaming**
- ✓ **Enhancement of the ϕ T cross-correlation in the case of the CMB lensing-potential, and for high redshift lensed sources, depending on the neutrino mass**
- ✓ **Suppression of ϕ T cross-correlation for low median redshift surveys, but anyway larger than $\phi \phi$ auto-correlation.**